General Disclaimer

One or more of the Following Statements may affect this Document

- This document has been reproduced from the best copy furnished by the organizational source. It is being released in the interest of making available as much information as possible.

- This document may contain data, which exceeds the sheet parameters. It was furnished in this condition by the organizational source and is the best copy available.

- This document may contain tone-on-tone or color graphs, charts and/or pictures, which have been reproduced in black and white.

- This document is paginated as submitted by the original source.

- Portions of this document are not fully legible due to the historical nature of some of the material. However, it is the best reproduction available from the original submission.

VORTEX MOTION IN AXISYMMETRIC PISTON-CYLINDER CONFIGURATIONS

T.I.P. Shih, G.E. Smith and G.S. Springer

/September 1982/

Backup Document for AIAA Synoptic Scheduled for Publication in the AIAA Journal, March 1984

212 MEB
Department of Mechanical Engineering
University of Florida
Gainesville, FL 32611

VORTEX MOTION IN AXISYMMETRIC PISTON-CYLINDER CONFIGURATIONS

by

Tom I-P. Shih*, Gene E. Smith+, and George S. Springer≠
The University of Michigan
An Arbor, Michigan

ABSTRACT

By using the Beam and Warming implicit-factored method of solution of the Navier-Stokes equations, velocities were calculated inside axisymmetric piston-cylinder configurations during the intake and compression strokes. Results are presented in graphicial form which show the formation, growth and break-up of those vortices which form during the intake stroke by the jet issuing from the valve. It is shown that at bore-to-stroke ratio of less than unity, the vortices may break-up during the intake stroke. It is also shown that vortices which do not break-up during the intake stroke coalesce during the compression stroke.

*Graduate Student, Department of Mechanical Engineering and Applied Mechanics; presently, Aerospace Engineer, NASA-Lewis Research Center, Cleveland, Ohio; Member AIAA

+Professor, Department of Mechanical Engineering and Applied Mechanics

≠Professor, Department of Mechanical Engineering and Applied Mechanics, Assoc. Fellow AIAA

I. INTRODUCTION

Fluid motion inside cylinders of reciprocating piston engines has been studied both by experimental (1 - 12) and analytical (13 - 34) methods. These investigations have revealed that recirculating flows (vortices) form during the intake stroke by the jet issuing from the intake valve. Under some conditions these vorticies may persist throughout the compression stroke (32) and seriously affect the ignition and flame propagation processes. Since these vortices can play such an important role in the combustion process, their formation, growth, and break-up during the intake stroke, and their subsequent behavior during the compression stroke must be understood. However, most of the previous studies focused only on the problem of vortex motion during the intake stroke. In spite of the importance of the problem, relatively little is known about the behavior of vortices during the compression stroke. This investigation was addressed therefore to the study of vortex motion during the compression stroke of those vortices which form during the intake stroke. To accomplish this, velocities were calculated inside axisymmetric piston-cylinder configurations. The velocity fields were presented in graphical forms which illustrate the formation, growth, and break-up of the vortices.

II. DESCRIPTION OF THE PROBLEM

The following problem was analyzed. A hollow circular cylinder is closed on one end by a flat piston and on the other end by a flat plate (Fig. 1). The piston is connected to a crank shaft through a connecting rod. The piston is driven by rotation of the crank shaft about the crank pin at an angular velocity Ω, resulting in a piston velocity u_p.

The flat plate has a centrally located annular opening (valve opening) in it which opens instantaneously at the beginning of the intake stroke (crank angle $\phi = 0$) and closes instantaneously at the end of the intake stroke ($\phi = \pi$).

The temperatures at the cylinder wall T_w, valve T_v, cylinder head T_h, and piston T_p are constants, but may have different values.

The fluid enters the piston-cylinder configuration described above through the valve opening during the intake stroke. The stagnation temperature T_i and stagnation pressure P_i of the entering fluid are both taken to be constants. At the valve opening (seat angle α), the entering fluid may have velocity components in the radial (V_r) and axial (V_z) directions, but not in the tangential direction. The magnitude of the velocity at the valve opening depends upon the instantaneous flow field inside the cylinder as well as the stagnation temperature and pressure of the entering fluid.

The viscous and thermally conducting fluid which enters the cylinder is an ideal gas having constant thermodynamic and transport properties.

At the beginning of the intake stroke, the gas in the clearance volume (residual gas) is taken to be a stagnant, ideal gas at stagnation temperature T_i and stagnation pressure P_c ($P_c \leq P_i$). The residual gas has the same thermodynamic and transport properties as the intake charge.

III. METHOD OF SOLUTION

The basic equations governing the problem are the conservation equations of mass, radial momentum, axial momentum, and energy (35). To render these equations more amenable to numerical methods of solution, body forces were neglected and the bulk viscosity was taken to be zero.

The governing equations, applicable to laminar flows, are summarized in Table 1. Turbulence was taken into account by the method described subsequently. Equations 1 - 13 (Table 1) constitute a closed system in the four basic dependent variables: density (ρ), radial velocity (V_r), axial velocity (V_z), and energy (e).

The boundary and initial conditions corresponding to Eqs. 1 - 13 are given in Table 2. The no-slip condition requires the fluid velocity next to a solid wall to be equal to the velocity of the solid wall (Eqs. 14 and 15). The gas temperature next to solid walls equals the temperature of the walls. With all walls maintained at constant temperatures, this boundary condition results in Eqs. 16 - 19.

The stagnation pressure and stagnation temperature of the gas at the valve opening are constant with respect to time as reflected by Eqs. 20 and 21. The radial and axial velocities at the valve opening are related, as indicated by Eq. 22. The axial velocity at the valve opening is determined by applying the conservation of mass equation at the valve opening (Eq. 23).

The symmetry conditions at the center line result in Eq. 24. At time t equal to zero, the piston is at the TDC position ($\phi = 0$) and the residual gas in the clearance volume is a stagnant, ideal gas at stagnation pressure P_c and stagnation temperature T_i. These initial conditions are specified by Eq. 25.

Recent evidence suggests that the type of turbulence model employed in the analysis does not affect significantly the calculated flow pattern (36). For this reason the increased mixing due to turbulence was simulated in a simple and convenient manner by choosing appropriate values of the effective transport properties.

It has been observed that the effective viscosity for turbulent flows inside spark ignition engine cylinders is roughly 100 times higher than the viscosity corresponding to laminar flows (37). Therefore, the viscosity, μ, was taken to be 100 times the viscosity of air. The valve of the thermal conductivity, λ, was selected by taking the turbulent Prandtl number ($P_r = \mu C_p/\lambda$) to be equal to unity (38, 39).

Solutions to the governing equations and the corresponding initial and boundary conditions formulated above must be obtained by numerical methods. In this investigation, the implicit-factored, finite-difference method of Beam and Warming (40, 41) was used to obtain solutions. The details of the method are not given here because of the very long description this would require. Readers interested in the solution procedure are referred to references 42 and 43 which contain detailed descriptions of the method, including the formulation of the finite-difference equations and numerical boundary conditions, and discussions of the grid sizes, time steps, stability criteria, and computer time.

IV. RESULTS

Calculations were performed to explore the vortex patterns inside the cylinder during the intake and compression strokes. The emphasis of this investigation was on the behavior of vortices during the compression stroke. However, vortex formation during the intake stroke was also examined, since it is these vortices which carry over into the compression stroke.

The ranges of the parameters for which numerical solutions were obtained are summarized in Table 3. The values of the parameters describing the geometry and operating conditions were selected so as to correspond to those typically found

in spark-ignition engines. The thermodynamic and transport properties were chosen so as to be physically reasonable and to permit the use of convenient grid sizes in the numerical solutions.

The axial and radial components of the gas velocities inside the cylinder were calculated as functions of time and for all the conditions listed in Table 3. In the interest of brevity, only typical results are presented here which illustrate the major features of the flow pattern. The resultant velocity vectors were plotted providing a picture of the flow pattern. These graphical results were deemed adequate for the purpose of this study which was to observe the flow pattern inside the cylinder.

Intake Stroke

During the intake stroke, two toroidal vortices were formed by the vorticity generated by the jet at the valve opening and by the adverse pressure gradients produced by the jet impinging on the piston surface (Figs. 2 and 3). One of these vortices was located between the jet and the cylinder wall (cylinder-head vortex). The other was located between the jet and the center line (valve vortex). The formation and subsequent motion of these vortices were found to be consistent with those observed in previous experimental (1 - 9) and numerical (15 - 30) studies.

However, the present results showed one phenomenon that has not been reported previously. At bore-to-stroke ratio of less than unity, the cylinder-head vortex broke up into two smaller vortices (Fig. 2). The break-up was caused by interaction of the valve and cylinder-head vortices. Ekchian and Hoult (1) also noted vortex break-up in their tests with water injected into a

circular cylinder. However, in Ekchian and Hoult's experiments, the vortex break-up was due to flow instability and not to vortex interaction. In Ekchian and Hoult's experiments the vortex broke up and then degenerated into a random flow. In the present study the vortex did not degenerate into a random flow because flow instability and three-dimensional flow (needed for the complete vortex break-up) were not included in the numerical solution.

Compression Stroke

During the intake stroke, the jet separated the cylinder-head and valve vortices minimizing the interaction between them (Figs. 2 and 3). During the compression stroke, the cylinder-head and valve vortices were no longer separated by the jet, allowing the two vortices to interact. Because of the rotational motion of the two vortices, they forced each other towards the piston. Since the two vortices were of unequal strength, the weaker one was pushed closer to the piston surface by the stronger one.

As the piston speed increased during the compression stroke (crank angle ϕ between 190 and 240 degrees), the two vortices began to coalesce (Fig. 4). The time of this coalescing depended upon the strength of the vortex which was nearer to the piston surface.

At crank angles ϕ between 230 and 240 degrees, the two vortices coalesced into a single toroidal vortex (Fig. 4). The coalescing of the cylinder-head and valve vortices has not been described by previous investigators. The disappearance of one vortex was found by Ashurst (18) and by Diwaker, et al (19) in numerical simulations of similar piston-cylinder problems.

Towards the end of the compression stroke (crank angle $\phi > 320$ degrees) a new recirculating flow (corner vortex) formed in the corner of the cylinder-head and cylinder wall (Fig. 4). The formation of the corner vortex has also been reported by Chong, et al (14) and Gosman, et al (29).

Finally, it is noted that in an actual cylinder, a vortex also forms near the cylinder wall due to the piston scraping off the boundary layer next to the cylinder wall during the compression stroke (10 - 12, 31, 32, 44 and 45). This vortex was not included in this study, since the interest here was only in those vortices which form during the intake stroke.

REFERENCES

1. Ekchian, A. and Hoult, D. P., "Flow Visualization Studies in an Internal Combustion Engine," SAE Paper No. 790095, 1979.

2. Gany, A., Larrea, J.-J., and Sirignano, W. A., "Laser-Doppler Velocimetry Measurements in a Motored I.C. Engine Simulator," AIAA Paper No. 80-0079, 1980.

3. Ramos, J. I., Gany, A., and Sirignano, W. A., "The Recirculating Flow Field in a Two-Stroke, Motored Engine: Comparison between Theory and Experiments," Momentum and Heat Transfer Processes in Recirculating Flows, HTD-Vol. 13, ASME, New York, 1980, pp. 63-69.

4. Ramos, J. I., Gany, A., and Sirignano, W. A., "Study of Turbulence in a Motored Four-Stroke Internal Combusion Engine," AIAA Journal, Vol. 19, 1981, pp. 595-600.

5. Morse, A. P., Whitelaw, J. H., and Yianneskis, M., "Turbulent Flow Measurements by Laser-Doppler Anemometry in Motored Piston-Cylinder Assemblies," Journal of Fluids Engineering, Vol. 101, 1979, pp. 208-217.

6. Morse, A., Whitelaw, J. H., and Yianneskis, M., "The Influence of Swirl on the Flow Characteristics of a Reciprocating Piston-Cylinder Assembly," Journal of Fluids Engineering, Vol. 102, 1980, pp. 478-480.

7. Bicen, A. F., Vlachos, N. S., and Whitelaw, J. H., "The Creation and Destruction of Vortices in Unsteady Flows," Letters in Heat and Mass Transfer, Vol. 7, 1980, pp. 77-82.

8. Morse, A. P. and Whitelaw, J. H., "Measurements of the In-Cylinder Flow of a Motored Four-Stroke Reciprocating Engine," Proc. Royal Society of London, Series A, Vol. 377, 1981, pp. 309-329.

9. Namazian, M., Hansen, S., Lyford-Pike, E., Sanchez-Barsse, J., Heywood, J., and Rife, J., "Schlieren Visualization of the Flow and Density Fields in the Cylinder of a Spark-Ignition Engine," SAE Paper No. 800044, 1980.

10. Matekunas, F. A., "A Schlieren Study of Combustion in a Rapid Compression Machine Simulating the Spark Ignition Engine," Paper Presented at the Seventeenth International Symposium on Combustion, University of Leeds, England, August 20-25, 1978.

11. Oppenheim, A. K., Chong, R. K., Teichman, K., Smith, O. T., Sawyer, R. F., Hom, K., and Stewart, H. E., "A Cinematographic Study of Combustion in an Enclosure Fitted with a Reciprocating Piston," Paper Presented at the Conference on Stratified Charge Engines, Institute of Mechanical Engineers, London, England, 1976.

12. Ishikawa, N. and Daily, J. W., "Observation of Flow Characteristics in a Model I.C. Engine Cylinder," SAE Paper 780230, 1978.

13. Boni, A. A., Chapman, M., and Schmeyer, G. P., "Computer Simulation of Combustion Processes in a Stratified Charge Engine," Acta Astronautica, Vol. 3, 1976, pp. 293-307.

14. Chong, M. S., Milkins, E. E., and Watson, H. C., "Predictions of Heat and Mass Transfer during Compression and Expansion in I.C. Engines," SAE Paper No. 760761, 1976.

15. Sod, G. A., "Automotive Engine Modeling with a Hybrid Random Choice Method," SAE Paper No. 790242, 1979.

16. Sod, G. A., "A Hybrid Random Choice Method with Application to Internal Combustion Engines II," LBL-9423, Lawrence Berkeley Laboratory, The University of California, Berkeley, 1979.

17. Sod, G. A., "Automotive Engine Modeling with a Hybrid Random Choice Method, II," SAE Paper No. 800288, 1980.

18. Ashurst, W. T., "Vortex Dynamic Calculation of Fluid Motion in a Four Stroke Piston 'Cylinder'-Planar and Axisymmetric Geometry," SAND 78-8229, Sandia Laboratories, Livermore, California, 1978.

19. Diwaker, R., Anderson, Jr., J. D., Griffin, M. D., and Jones, E., "Inviscid Solutions to the Flowfield in an Internal Combustion Engine," AIAA Journal, Vol. 14, 1976, pp. 1667-1668.

20. Griffin, M. D., Anderson, Jr., J. D., and Diwaker, R., "Navier-Stokes Solutions of the Flowfield in an Internal Combustion Engine," AIAA Journal, Vol. 14, 1976, pp. 1665-1666.

21. Griffin, M. D., Diwaker, R., Anderson, Jr., J. D., and Jones, E., "Computational Fluid Dynamics Applied to the Flow in an Internal Combustion Engine," AIAA Paper No. 78-57, January 1978.

22. Griffin, M. D., Anderson, Jr., J. D., and Jones, E., "Computational Fluid Dynamics Applied to Three-Dimensional Nonreacting Inviscid Flows in an Internal Combustion Engine," Journal of Fluids Engineering, Vol. 101, 1979, pp. 367-372.

23. Griffin, M. D., "Numerical Solutions for Two and Three-Dimensional Non-Reacting Flowfields in an Internal Combustion Engine," Ph.D. Thesis, University of Maryland, College Park, Maryland, 1977.

24. Ramos, J. I., Humphrey, J. A. C., and Sirignano, W. A., "Numerical Prediction of Axisymmetric Laminar and Turbulent Flows in Motored, Reciprocating Internal Combustion Engines," SAE Paper No. 790356, 1979.

25. Ramos, J.I., and Sirignano, W. A., "Axisymmetric Flow Model with and without Swirl in a Piston-Cylinder Arrangement with Idealized Valve Operation," SAE Paper No. 800284, 1980.

26. Ramos, J.I., and Sirignano, W. A., "Axisymmetric Flow Model in a Piston-Cylinder Arrangement with Detailed Analysis of the Valve Region," SAE Paper No. 800286, 1980.

27. Ramos, J. I., "Axisymmetric Flows in Spark-Ignition Engines," Report CO/80/2, Department of Mechanical Engineering, Carnegie-Mellon University, Pittsburgh, PA, 1980.

28. Ramos, J. I. and Sirignano, W. A., "Turbulent Flow Field in Homogeneous-Charge Spark-Ignition Engines," Eighteenth Symposium (International) on Combustion, The Combustion Institute, 1981, pp. 1825-1835.

29. Gosman, A. D., Johns, R. J. R., and Watkins, A. P., "Development of Prediction Methods for In-Cylinder Processes in Reciprocating Engines," in Combustion Modeling in Reciprocating Engines, J. N. Mattavi and C. A. Amann, eds., Plenum Press, New York, 1980, pp. 69-129.

30. Ahmadi-Befrui, B., Gosman, A. D., Lockwood, F. C., and Watkins, A. P., "Multidimensional Calculation of Combustion in an Idealized Homogeneous Charge Engine: A Progress Report," SAE Paper No. 810151, 1981.

31. Bernard, P. S., "Computation of the Turbulent Flow in an Internal Combustion Engine during Compression," Journal of Fluids Engineering, Vol. 103, 1981, pp. 75-81.

32. Witze, P. O., ed., "Comparisons between Measurement and Analysis of Fluid Motion in Internal Combustion Engines," SAND 81-8242, Sandia National Laboratories, Livermore, California, October 1981.

33. Boni, A. A., "Numerical Simulation of Flame Propagation in Internal Combustion Engines: A Status Report," SAE Paper No. 780316, 1978.

34. Butler, T. D., Cloutman, L. D., Dukowicz, J. K., and Ramshaw, J. D., "Multidimensional Numerical Simulation of Reactive Flow in Internal Combustion Engines," Progress in Energy and Combustion Sciences, Vol. 7, 1981, pp. 293-315.

35. Bird, R. B., Stewart, W. E., and Lightfoot, E. N., Transport Phenomena, John Wiley and Sons, Inc., New York, 1960.

36. Schock, H. J., Sosoka, D., and Ramos, J. I., "Numerical Studies of the Formation and Destruction of Vortices in a Four-Stroke Piston-Cylinder Configuration," Submitted to the AIAA Aerospace Sciences Meeting (1983).

37. Johnson, S. C., Robinson, C. W., Rorke, W. S., Smith, J. R., and Witze, P. O., "Application of Laser Diagnostics to an Injected Engine," SAE Paper No. 790092, 1979.

38. Launder, B. E. and Spalding, D. B., Lectures in Mathematical Models of Turbulence, Academic Press, London, 1972, pp. 46-70.

39. Reynolds, A. J., "The Prediction of Turbulent Prandtl and Schmidt Numbers," International Journal of Heat and Mass Transfer, Vol. 18, 1975, pp. 1055-1069.

40. Warming, R. F. and Beam, R. M., "On the Construction and Application of Implicit Factored Schemes for Conservation Laws," Symposium on Computational Fluid Dynamics, SIAM-AMS Proceedings, Vol. 11, H. B. Keller, ed., American Mathematical Society, Providence, Rhode Island, 1978, pp. 85-129.

41. Beam, R. M. and Warming, R. F., "An Implicit Factored Scheme for the Compressible Navier-Stokes Equations," AIAA Journal, Vol. 16, 1978, pp. 393-402.

42. Shih, T. I-P., "Application of the Implicit Factored Method to Complex Flow Problems," Ph.D. Thesis, Department of Mechanical Engineering and Applied Mechanics, The University of Michigan, Ann Arbor, Michigan, 1981.

43. Shih, T. I-P., Smith, G. E., Springer, G. S., and Rimon, Y., "Boundary Conditions for the Solution of Compressible Navier-Stokes Equations by an Implicit Factored Method," Journal of Computational Physics (submitted).

44. Tabaczynski, R. J., Hoult, D. P., and Keck, J. C., "High Reynolds Number Flow in a Moving Corner," Journal of Fluid Mechanics, Vol. 42, 1970, pp. 249-255.

45. Daneshyar, H., Fuller, D. E., and Deckker, B. E. L., "Vortex Motion Induced by the Piston of an Internal Combustion Engine," International Journal of Mechanical Sciences, Vol. 15, 1973, pp. 381-390.

LIST OF FIGURES

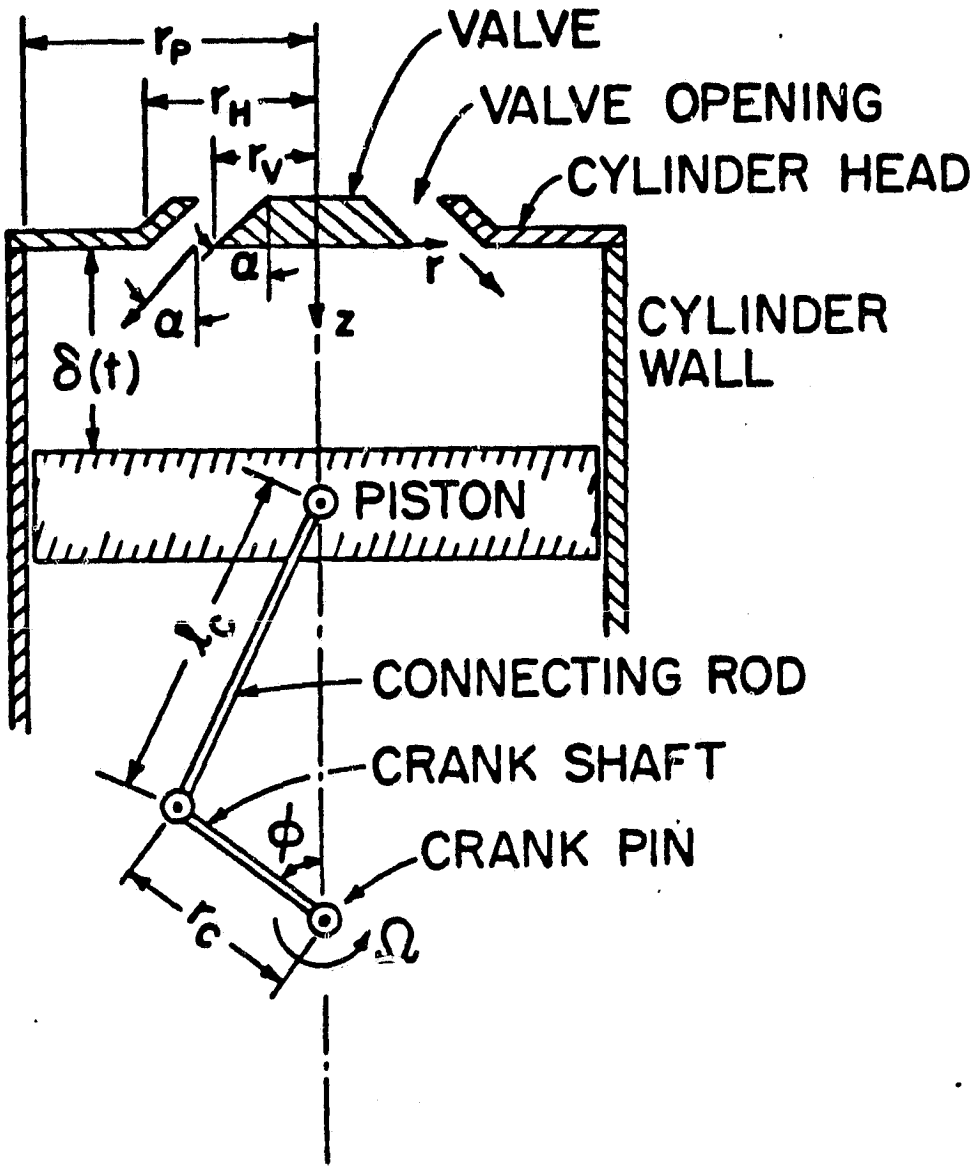

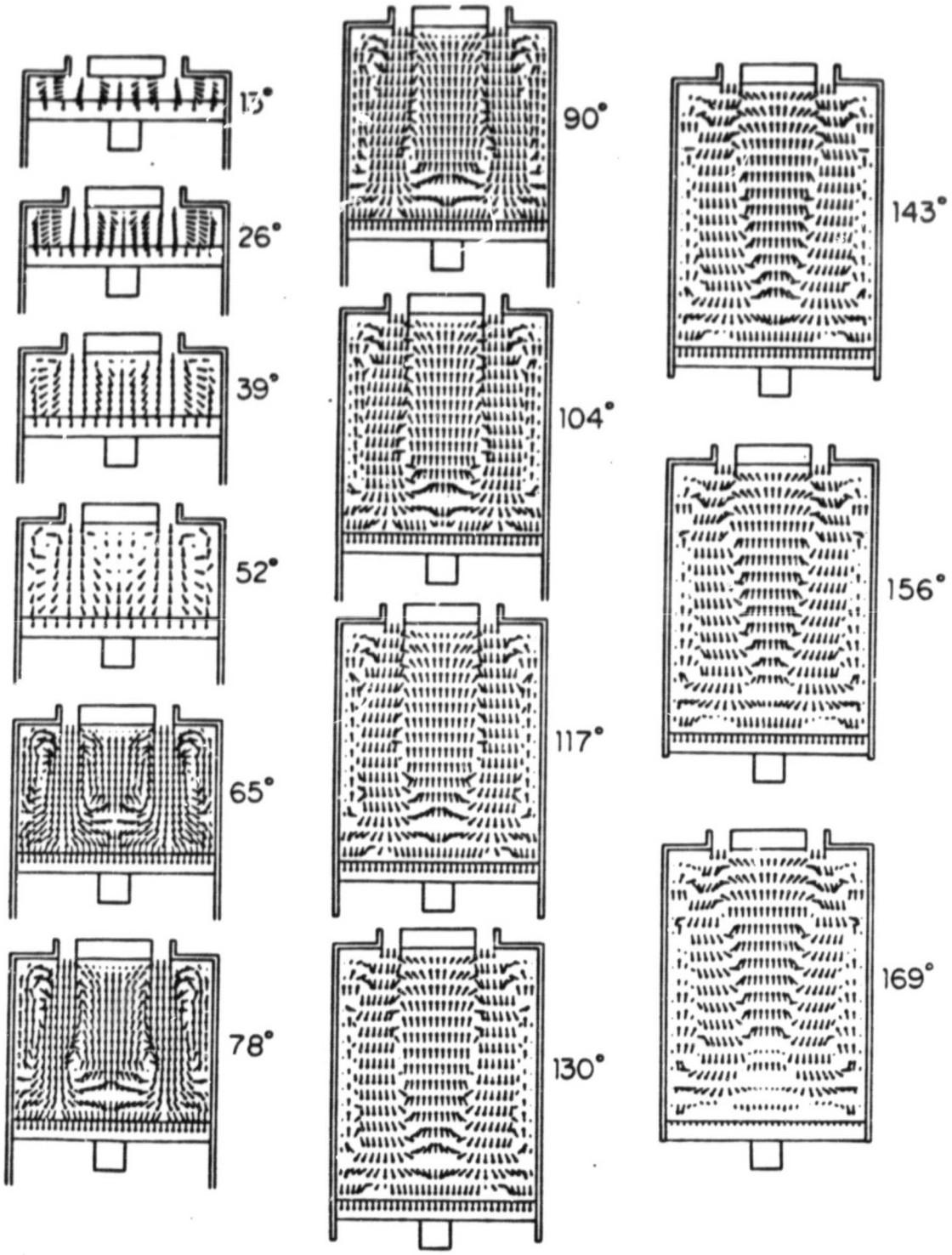

Fig. 02

Shih, Smith, and Spunger

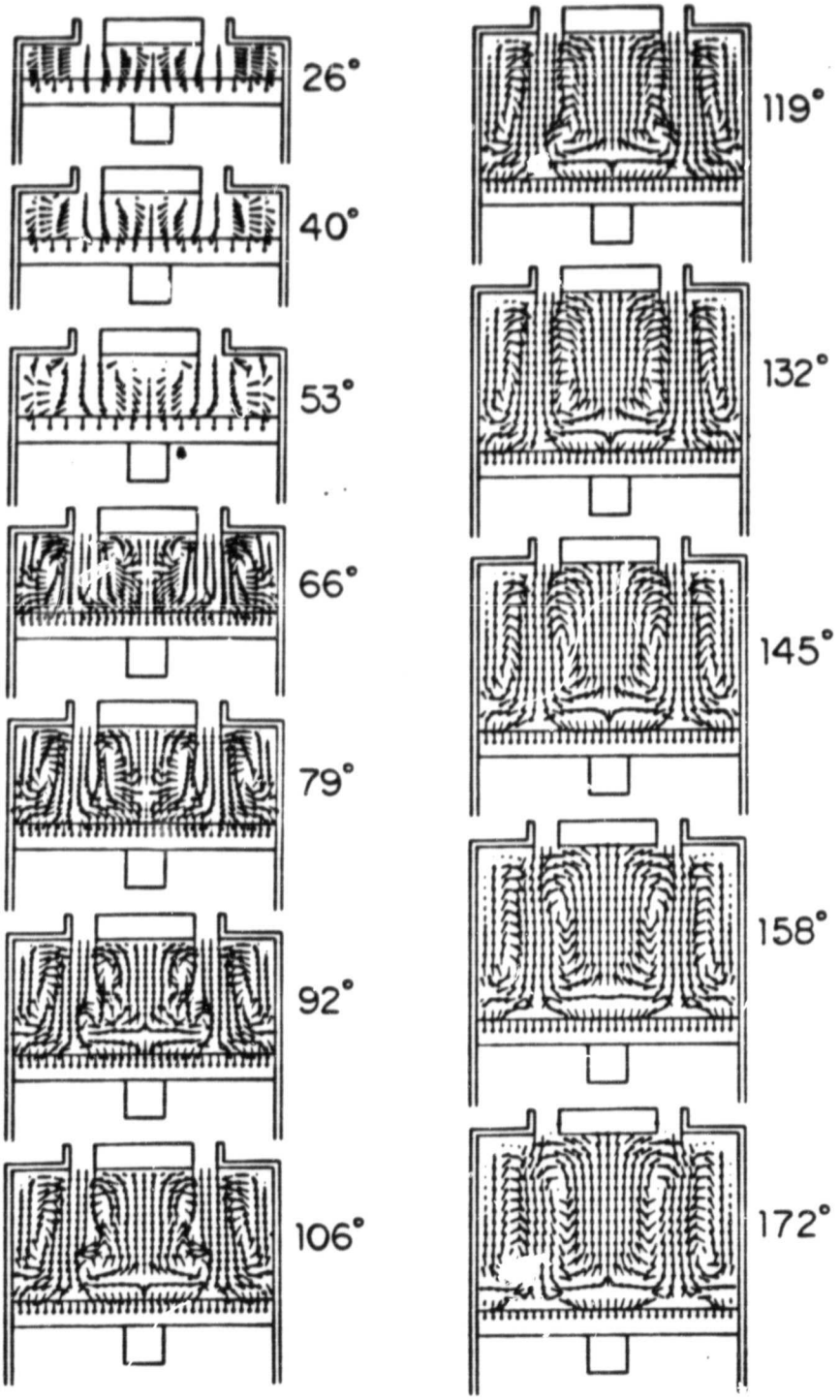

Fig. 3

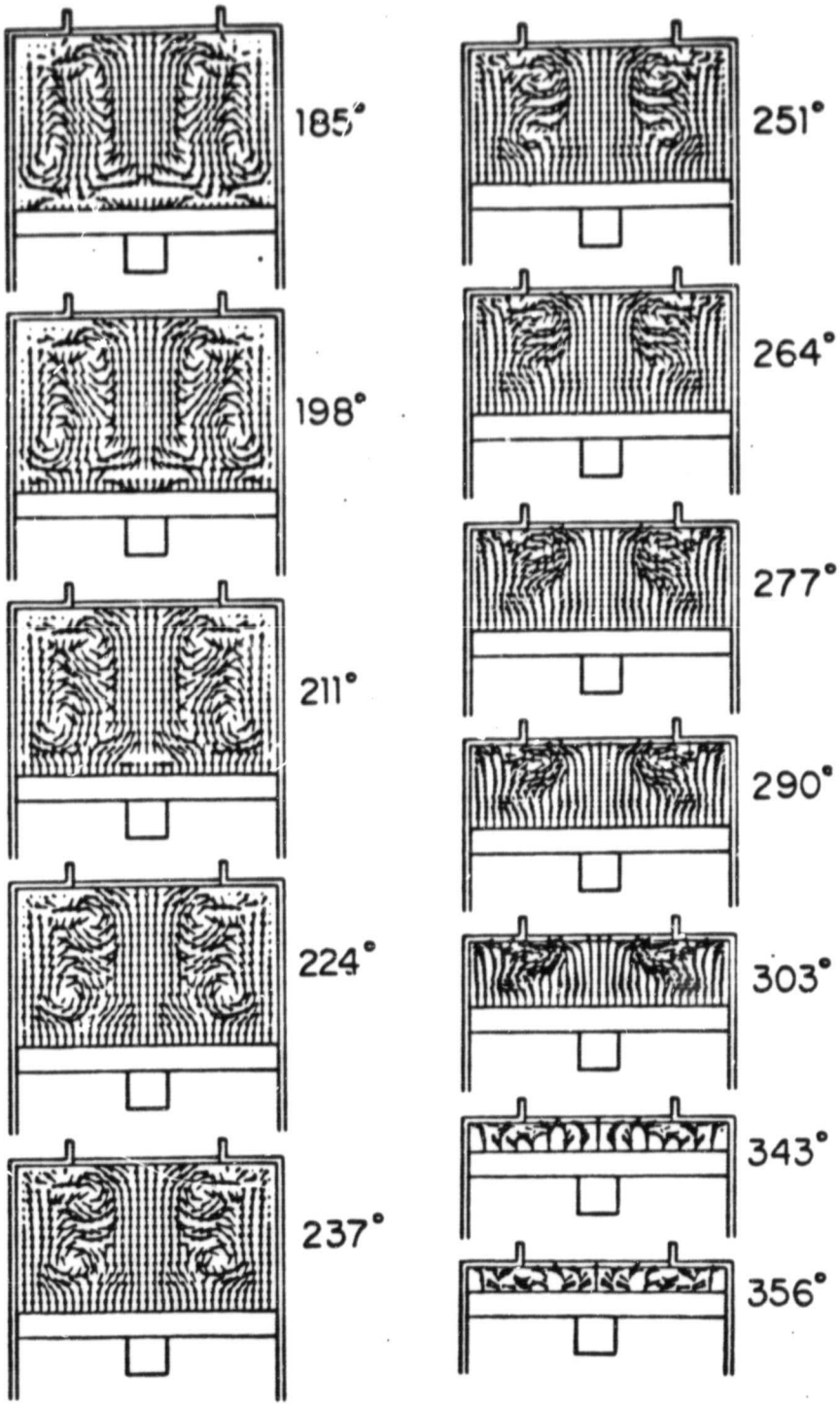

Fig. 4

Shih Smith & Lourenco

TABLE 1. GOVERNING EQUATIONS*

Equation	Eq. No.
$\frac{\partial \rho}{\partial t} + \frac{1}{r}\frac{\partial}{\partial r} r\rho V_r + \frac{\partial}{\partial z}\rho V_z = 0$	1
$\frac{\partial}{\partial t}\rho V_r + \frac{1}{r}\frac{\partial}{\partial r} r\rho V_r^2 + \frac{\partial}{\partial z}\rho V_r V_z = -\frac{\partial P}{\partial r} + \frac{1}{r}\frac{\partial}{\partial r} r\tau_{rr} - \frac{\tau_{\theta\theta}}{r} + \frac{\partial}{\partial z}\tau_{rz}$	2
$\frac{\partial}{\partial t}\rho V_z + \frac{1}{r}\frac{\partial}{\partial r} r\rho V_r V_z + \frac{\partial}{\partial z}\rho V_z^2 = -\frac{\partial P}{\partial z} + \frac{1}{r}\frac{\partial}{\partial r} r\tau_{rz} + \frac{\partial}{\partial z}\tau_{zz}$	3
$\frac{\partial e}{\partial t} + \frac{1}{r}\frac{\partial}{\partial r} r(e+P)V_r + \frac{\partial}{\partial z}(e+P)V_z = \frac{1}{r}\frac{\partial}{\partial r} r(\tau_{rr}V_r + \tau_{rz}V_z) + \frac{\partial}{\partial z}(\tau_{rz}V_r + \tau_{zz}V_z) - \frac{1}{r}\frac{\partial}{\partial r} r q_r - \frac{\partial}{\partial z} q_z$	4
$\tau_{rr} = 2\mu\frac{\partial V_r}{\partial r} - \frac{2}{3}\mu(\nabla\cdot\vec{V})$	5
$\tau_{\theta\theta} = 2\mu\frac{V_r}{r} - \frac{2}{3}\mu(\nabla\cdot\vec{V})$	6
$\tau_{zz} = 2\mu\frac{\partial V_z}{\partial z} - \frac{2}{3}\mu(\nabla\cdot\vec{V})$	7
$\tau_{rz} = \mu\left(\frac{\partial V_r}{\partial z} + \frac{\partial V_z}{\partial r}\right)$	8
$\nabla\cdot\vec{V} = \frac{1}{r}\frac{\partial}{\partial r} r V_r + \frac{\partial V_z}{\partial z}$	9
$h = h^\circ + \int_{T_i}^{T} C_p\, dT = h^\circ + C_p(T - T_i)$	10
$q_r = -\lambda\frac{\partial T}{\partial r}$	11
$q_z = -\lambda\frac{\partial T}{\partial z}$	12
$P = \rho\frac{R}{M}T$	13

* C_p = constant pressure specific heat, e = energy per unit volume, h = specific enthalpy, h° = standard enthalpy of formation per unit mass at temperature T_i, M = molecular weight, P = static pressure, q_j = heat flux in the j-direction, R = universal gas constant, V_j = j-component of the velocity, λ = thermal conductivity, μ = viscosity, ρ = density, τ = shear stress.

TABLE 2. BOUNDARY AND INITIAL CONDITIONS

Equation		Eq. No.
$V_r = 0$, $V_z = U_p$	piston surface	14
$V_r = V_z = 0$	cylinder head, cylinder wall, and valve	15
$T = T_v$	valve	16
$T = T_h$	cylinder head	17
$T = T_w$	cylinder wall	18
$T = T_p$	piston surface	19
$P = P_i \left(\frac{T}{T_i}\right)^{\frac{\gamma}{\gamma-1}}$, $\gamma = C_p/(C_p - R/M)$	valve opening	20
$T = T_i - \frac{(V_r^2 + V_z^2)/2}{C_p}$	vavle opening	21
$V_r = V_z \tan \alpha$	valve opening	22
$\frac{\partial \rho}{\partial t} + \frac{1}{r}\frac{\partial}{\partial r} r \rho V_r + \frac{\partial}{\partial z} \rho V_z = 0$	valve opening	23
$\frac{\partial \rho}{\partial r} = V_r = \frac{\partial V_z}{\partial r} = \frac{\partial e}{\partial r} = 0$	center line	24
$\rho = P_i/(RT_i/M)$, $V_r = V_z = 0$ $e = P_i\left[(MC_p - R)/R + (h^o - C_p T_i)\right]$	everywhere inside the piston-cylinder configuration at time t = 0	25

TABLE 3. SUMMARY OF PARAMETERS USED IN THE NUMERICAL CALCULATIONS*

r_p/r_c	(rpm)	P_i/P_c	α(degrees)
0.78	400	1	0
1.67	400	1	0
1.67	400	1.036	0
1.67	400	1	45
1.67	400	1	0

* The following parameters were the same for all cases studied: $\mu = 3.2 \times 10^{-3}$ kg/m-s, $\lambda = 3.224$ kg-m/s^2 - °K, $h = 42{,}252$ m^2/s^2, $C_p = 1{,}006.6$ m^2/s^2 - °K, M = 28.96 kg/kg-mole, R = 8314.3 kg-m^2/ kg-mole-°K-s, r_p = 0.05 m, r_v = 0.01875 m, r_H = 0.03438 m, $\delta(t=0)$ = 0.01 m, l_c = 0.2m, $T_i = T_v = T_h = T_w = T_p = 340$ K, and $P_c = 101325$ kg/m-s^2. Results are shown only for the first two cases listed in this table.